Distributed Acoustic Sensing for Datacenter Optical Interconnects using Self-Homodyne Coherent Detection

Ezra Ip[1], Yue-Kai Huang[1], Ting Wang[1], Yoshiaki Aono[2] and Koji Asahi[2]

[1] NEC Laboratories America, Princeton, NJ, USA, [2] 1st Network Solution Division, NEC Corporation, Japan

E-mail address: ezra.ip@nec-labs.com

Abstract: We demonstrate distributed acoustic sensing (DAS) over a bidirectional datacenter link which uses self-homodyne coherent detection for the data signal. Frequency multiplexing allows sharing the optoelectronic hardware, and enables DAS as an auxiliary function. © 2021

1. Introduction

Optical fiber sensing has become an important tool for network operators to manage their infrastructure assets and to provide additional revenue opportunities. Wide-ranging applications including traffic monitoring, intrusion detection, infrastructure health monitoring and earthquake detection contribute to public safety and smarter cities in metro, long-haul, and submarine networks [1]. For datacenter interconnect (DCI), fiber sensing can be a useful network diagnostic tool and for intra-building monitoring, and is facilitated by large numbers of available fibers. However, solutions have to be low-cost and be compatible with the network architecture and transmission formats used in DCI. Although it has been shown that state of polarization (SOP) and optical phase can both be extracted from telecom transponders for vibration sensing [2,3], these techniques cannot provide the location accuracy needed for DCI sensing applications.

Self-homodyne detection was recently proposed as a solution for DCI where fibers are abundant, component bandwidth is a limiting factor, and the data rate per channel can be increased through higher spectral efficiency realized at reasonable digital signal processing (DSP) cost using reduced-complexity coherent receivers [4,5]. As this scheme requires that the data signal and local oscillator (LO) are transmitted over two parallel fibers, the bidirectional architecture can be exploited for DAS. In this paper, we show that by appropriate spectral arrangement and with minimal additional hardware, a sensing signal can be multiplexed with the data signal at the transmitter, and the Rayleigh backscatter can be detected using the same coherent receiver as the data signal, enabling the realization of DAS as an auxiliary function at low cost. We demonstrate our scheme for bidirectional 200-Gb/s DP-16QAM signals while simultaneously achieving DAS at 13 m resolution at a sensitivity $< 20\ \mathrm{p}\epsilon/\sqrt{\mathrm{Hz}}$.

2. Principles of Operation

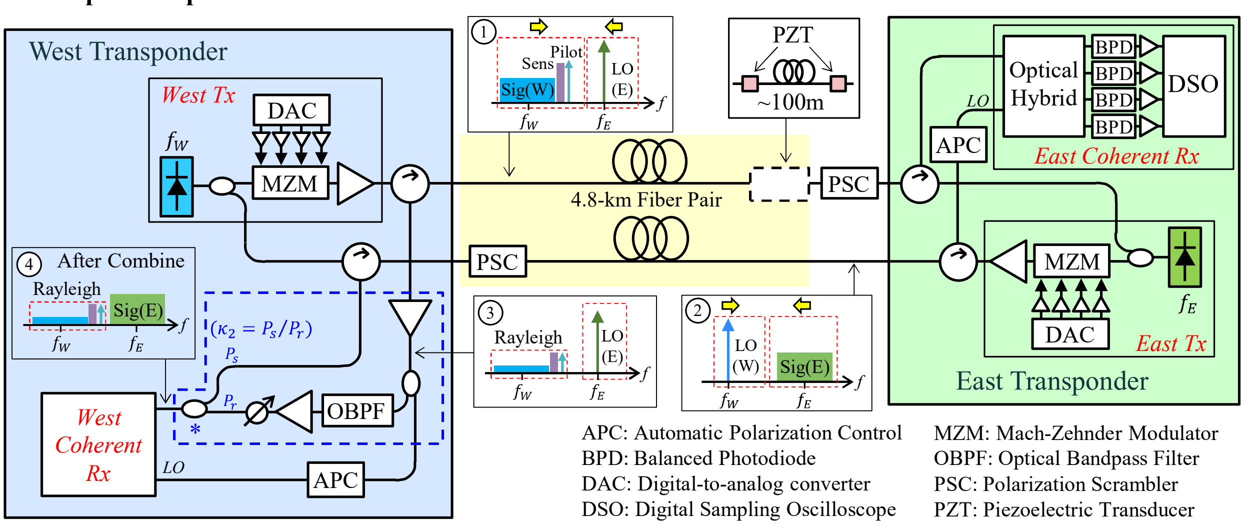

Fig. 1. Experimental setup for DAS-compatible DCI with self-homodyne coherent detection for both data signals.

The principle of our DAS-compatible DCI and experimental setup is shown in Fig. 1. Bidirectional data transmission between East (E) and West (W) transponders with self-homodyne coherent detection is facilitated by two fibers. In the top fiber, the West signal propagates to the right while the East LO propagates to the left, as shown by the spectrum in Inset 1 of Fig. 1. In the bottom fiber, the West LO propagates to the right while the East signal propagates to the left (Inset 2). Each transponder uses digital-to-analog converters (DACs) and Mach-Zehnder modulators (MZM) to generate their transmitted signals, while for the receiver, each transponder performs self-homodyne coherent detection by beating the received signal on one fiber with the received LO on the other fiber. To ensure the LO is aligned with the reference polarization of the optical hybrid, active polarization controllers (APC) are used. Signals are launched and received from the fiber pair via circulators. To facilitate DAS, we spectrally multiplexed a sensing signal with the data signal at the West transmitter. As the bandwidth of the sensing signal, typically on the order of tens of MHz, is much less than the baud rate of the data signal, and the frequency responses of optoelectronic components have gradual roll-off, it is possible to (i) use the same DACs to generate both data and sensing signals, and (ii) use the same coherent receiver front-end to simultaneously demodulate the East data signal and the Rayleigh backscatter of the West sensing signal. The blue dotted box inside the West transponder in Fig. 1 shows the extra optical components needed to realize the DAS function. At the drop port of the top-left circulator, the signal is amplified and split. Since Rayleigh backscatter has much lower power than the East LO (Inset 3), we can inject it directly into the LO port of the coherent receiver after passing it through the APC; the Rayleigh backscatter only results in a slightly noisy LO. At the other splitter output, an optical bandpass filter (OBPF) suppresses the East LO with high extinction ratio while passing the Rayleigh backscatter. In our experiment, the OBPF was realized using two concatenated fiber Bragg grating (FBG) filters with 20-GHz bandwidth. The OBPF output is amplified, followed by combining with the East signal using a passive coupler. The combined signal (Inset 4) is injected into the signal port of the West coherent receiver. In this architecture, the data signals are detected using self-homodyne coherent detection, whereas the Rayleigh backscatter is detected using intradyne detection, since the sensing signal was generated using the West laser but is demodulated by the East LO. Intradyne detection is susceptible to laser phase noise, particularly at low-frequencies which manifests as frequency drift between the East and West lasers, causing their intermediate frequency $\Delta f = f_W - f_E$ to be time-varying. As DAS measures time-varying phase change, laser phase noise will degrade performance. To mitigate this, we transmit a pilot tone alongside the sensing signal as shown in Inset 1. This pilot assists the West receiver to locate and correctly demodulate the received Rayleigh backscatter of the sensing signal using correlation detection.

3. Experimental Setup and Results

We generated 32-Gbaud DP-16QAM with 5% raised-cosine (RC) pulse shaping using a 64-GSa/s DAC. For the sensing signal, we used chirped pulses of bandwidth $R = 15.625$ MHz and duration of 2.048 μs, at a repetition rate of $R_p = 20.35$ kHz (maximum interrogation distance ~ 5.1 km) [6]. The sensing signal was centered about 16.3 GHz, while a pilot tone at 5 dB lower power than the sensing signal was inserted at 16.7 GHz. External cavity lasers (ECL) with linewidths around 30 kHz and center frequencies of 193.4000 THz and 193.4332 THz are used for the West and East lasers, respectively. Dithering was turned off to provide improved frequency stability for DAS. The top figure in Fig. 2(a) shows the electrical spectrum measured by the East coherent receiver over a 4 μs interval containing the chirped sensing signal. The link comprises of two 4.8-km spools of standard single-mode fiber (SSMF). A polarization scrambler (PSC) is inserted as shown in Fig. 1 to allow evaluation of performance degradation arising from PSC and APC. The power of the signal and LO at launch (measured at the output of the circulator) are both set to +10 dBm. While a lower launch power can be used for the East signal, a high power is needed for the West signal to generate a sufficiently strong Rayleigh reflection. Integrated coherent receivers (ICR) are used to demodulate the received signal with the received LO. The ICR outputs are sampled and digitized using a 50-GSa/s digital sampling oscilloscope (DSO). The E-W and W-E directions are measured separately. The DSO is operated in sequential data capture mode at a rate of R_p. Each frame has a duration of 4 μs (200,000 samples). Memory limitation restricted the number frames captured to 155, thus our DAS has a frequency resolution of $20350/155 = 131$ Hz. For offline DSP, we follow the approach in [4] which omits carrier phase recovery to reduce DSP complexity. Difference in path length between the top and bottom fibers will cause slight rotation of the received constellation due to laser phase noise. This is compensated by optimizing the step size of the real-valued 4×4 adaptive time-domain equalizer (TDE) [4]. For the DAS, the Rayleigh impulse response of the top fiber is recovered using correlation detection. Differential beat terms are then calculated at time difference of $\tau_g = 2/R = 0.128$ μs, corresponding to a spatial resolution of 13.3 m.

We first optimize the power ratio κ_1 between the data and sensing signals generated by the West transponder. The presence of the sensing signal reduces the effective number of bits (ENOB) available for the data signal at both DAC and ADC, causing reduction in back-to-back signal-to-noise ratio (SNR). However, setting the power of the sensing signal too low will degrade the optical SNR of the DAS. Fig. 2(b) shows $\mathrm{BER_W}$ vs TDE length (N_{tap}). As expected, reducing N_{tap} or κ_1 degrades $\mathrm{BER_W}$. At $\kappa_1 = 21$ dB and $N_{tap} = 7$, a BER below the KP4 forward-error correction (FEC) threshold of 2.2×10^{-4} was achieved [7]. With the West signal fixed at $\kappa_1 = 21$ dB, and the East signal having no sensing signal or pilot (Inset 2 of Fig. 1), we next optimize the power ratio κ_2 between the received East signal and the Rayleigh backscatter at the coupler marked (*) in Fig. 1. As amplified spontaneous emission (ASE) noises in the two paths add, a larger κ_2 will improve the $\mathrm{BER_E}$ at the potential expense of DAS sensitivity, and vice versa. The bottom figure in Fig. 2(a) shows electrical spectra measured at the West coherent receiver for two values of κ_2. At low κ_2, noise on the left-side of the spectrum is increased due to ASE in the Rayleigh path. Fig. 2(c) shows $\mathrm{BER_E}$ and phase noise power spectral density (PSD) of the DAS vs κ_2. Reducing κ_2 results in worse $\mathrm{BER_E}$. However, phase noise PSD shows little variation with κ_2 as the optical SNR of the DAS is set by the amplifier before the OBPF. This is observed in Fig. 2(a) where the Rayleigh reflection of the sensing signal is always ~ 15 dB above the noise level. The average phase noise PSD of ~4×10^{-6} $\mathrm{rad^2/Hz}$ corresponds to a DAS sensitivity of ~17 $\mathrm{p\epsilon/\sqrt{Hz}}$.

To demonstrate correct operation of the DAS, two 12-m long piezoelectric transducers (PZT) separated by ~100 m of fiber was inserted just before the PSC in the top fiber (Fig. 1), and their frequencies are set to 1,866 and 1,267 Hz, respectively. Fig. 2(d) shows the measured phase spectrum vs distance. The color of each pixel denotes vibration energy (in units of dBc/Hz) at that frequency. The two PZTs can be seen clearly at 4,810 and 4,929 m. Fig. 2(e) shows the phase spectra at these locations. Finally, we measured the BER vs received power characteristic for both West ($\kappa_1 = 21$ dB) and East data signals ($\kappa_2 = 15$ dB). Fig. 2(f) shows results for back-to-back (BTB), and after transmission. The West data is always worse due to the presence of the sensing signal, while performance degrades only slightly with transmission and PSC/APC.

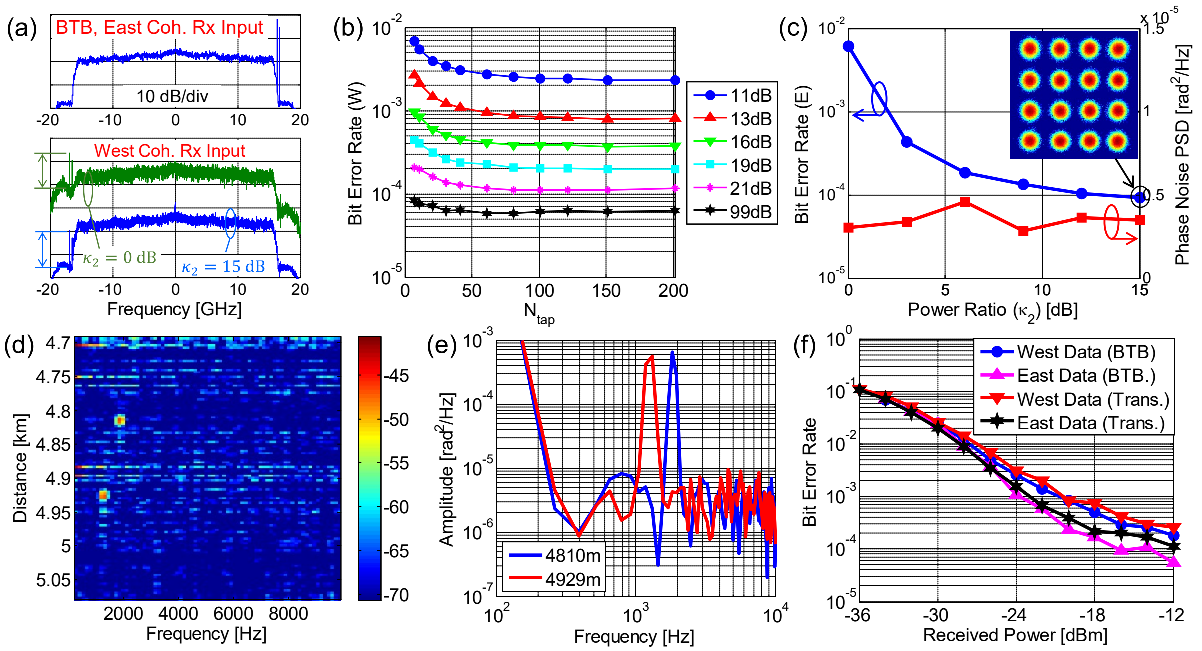

Fig. 2. Experimental results. (a) Spectra at East and West coherent receivers after optical-to-electrical downconversion, (b) $\mathrm{BER_W}$ vs DSP complexity for different power ratios κ_1, (c) $\mathrm{BER_E}$ and Phase noise PSD of DAS vs κ_2, (d) Phase spectrum vs distance, (e) Phase spectra at the location of the two PZTs, (f) BER vs received power for West and East data signals, BTB and after transmission (with PSC and APC).

4. Conclusions

We have demonstrated a DAS-compatible bidirectional DCI scheme using self-homodyne coherent detection. Making use of the gradual frequency roll-off in optoelectronic devices, the sensing signal and its Rayleigh back-reflection are generated and detected using the same DACs and ADCs as the data signal. A pilot tone was inserted to assist the removal of laser phase noise from the DAS measurement. With optimization of the power ratios between data and sensing signals (and its Rayleigh backscatter) at the transmitter and receiver, we achieved 200-Gb/s DP-16QAM transmission at BER below the KP4 threshold, and DAS sensitivity < 20 $\mathrm{p\epsilon/\sqrt{Hz}}$ at a spatial resolution of 13.3 m.

5. References

[1] P. Lu et al., "Distributed optical fiber sensing: Review and perspective," Appl. Phys. Review, **6**(4), 041302 (2019).
[2] Z. Zhan et al., "Optical polarization–based seismic and water wave sensing on transoceanic cables," *Science*, **371**(6532), 931-936, (2021).
[3] G. Well brock et al., "Field trial of vibration detection and localization using coherent telecom transponders over 380-km link," Optical Fiber Conference (OFC 2021), Paper F3B.2, San Francisco, USA (2021).
[4] M. Sowailem et al., "Self-homodyne system or next-generation intra-datacenter optical interconnects," Opt. Exp. **25**(22), 27834–44 (2017).
[5] L. Wang et al., "First real-time MIMO-free 800 Gb/s DP-64QAM demonstration using bi-directional self-homodyne coherent transceiver," Optical Fiber Conference (OFC 2021), Paper Th3.C.2, San Francisco, CA, USA (2021).
[6] S. Wang et al., "Distributed fiber-optic vibration sensing based on phase extraction from time-gated digital OFDR," Opt. Exp. **23**(26), 33301–33309 (2015).
[7] S. Bhoja et al., "FEC codes for 400 Gbps 802.3bs," IEEE P802.3bs 400 GbE Task Force, Plenary meeting material, Macau (2014). Available: http://www.ieee802.org/3/bs/public/14_11/parthasarathy_3bs_01a_1114.pdf.